ACS OMEGA

http://pubs.acs.org/journal/acsodf

Article

Investigation of Small-Molecule Constituents in *Voacanga africana* Seeds and Mapping of Their Spatial Distributions Using Laser Ablation Direct Analysis in Real-Time Imaging–Mass Spectrometry (LADI-MS)

Allix Marie Coon and Rabi Ann Musah*

Cite This: *ACS Omega* 2023, 8, 27190–27205

Read Online

ACCESS | Metrics & More | Article Recommendations | Supporting Information

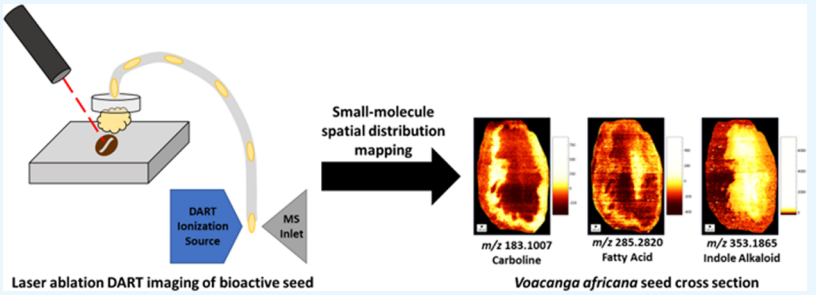

ABSTRACT: Plant seeds are a renewable resource that can furnish access to medicinal natural products that can only otherwise be isolated from aerial or root parts, the harvest of which may be destructive to the plant or threaten its viability. However, optimization of the isolation of such compounds from seeds would be greatly assisted if the spatial distribution of the molecules of interest within the plant tissue were known. For example, iboga alkaloids that hold promise for the treatment of opioid use disorder are typically isolated from the leaves, bark, or roots of *Tabernanthe* or *Voacanga* spp. trees, but it would be more environmentally sustainable to isolate such compounds from their seeds. Here, we leveraged the unique capabilities of the ambient mass spectral imaging technique termed laser ablation direct analysis in real-time imaging–mass spectrometry (LADI-MS) to reveal the spatial distributions of a range of molecules, including alkaloids within *V. africana* seeds. In addition to six compounds previously reported in these seeds, namely, tetradecanoic acid, *n*-hexadecanoic acid, (*Z*,*Z*)-9,12-octadecadienoic acid, (*Z*)-9-octadecenoic acid, octadecanoic acid, and Δ^{14}-vincamine, an additional 31 compounds were newly identified in *V. africana* seeds. The compound classes included alkaloids, terpenes, and fatty acids. The ion images showed that the fatty acids were localized in the embryo of the seed. The alkaloids, which were mainly localized in the seed endosperm, included strictamine, akuammidine, polyneuridine, vobasine, and Δ^{14}-vincamine. This information can be exploited to enhance the efficiency of secondary metabolite isolation from *V. africana* seeds while eliminating the destruction of other plant parts.

INTRODUCTION

Indole alkaloid natural products are ubiquitous secondary metabolites that are produced by plants, animals, and microbes. They range in form from simple endogenous central nervous system (CNS)-active signaling molecules, such as serotonin, to exquisitely complex molecular scaffolds such as villalstonine,[1] paraherquamide J,[2] and the mangrovamides D–G.[3] Plants in particular, both terrestrial and marine, serve as a rich source of these compounds, with many well-known examples that are used clinically, such as the anti-cancer drugs vincristine, vinblastine, vinflunine, and vinorelbine derived from the plant *Catharanthus roseus*. Their skeletal frameworks and biological activity have also inspired the synthesis of various lead drug candidates[4,5] and various synthetic approaches for their generation.[5] However, their structural complexity and stereochemical intricacy make them difficult to synthesize, and overall, their inaccessibility and the scarcity of the biological resources from which they are derived limit exploration of their biological properties that may be of therapeutic benefit, even when these properties appear promising for the treatment of disease. One case in point are the indole alkaloids derived from *Tabernanthe*[6] and *Voacanga*[7] genus plants, from which ibogaine, a compound that holds promise for the treatment of opioid and other chemical addictions,[7−9] has been isolated. While there are approaches to

Received: April 11, 2023
Accepted: June 14, 2023
Published: July 18, 2023

the synthesis of ibogaine,[10−14] these remain costly, and furthermore, the scheduling of ibogaine in the United States has stymied efforts to conduct studies of its potential as an anti-addiction treatment. *Tabernanthe* and *Voacanga* spp. also contain numerous other related but currently unregulated compounds, which have CNS activity that may be useful for the treatment of drug addiction. However, the lack of availability of these molecules in purified form has hampered efforts to study their potential utility.

Indole alkaloids with biological activity that have been isolated from the plant include voafolidine from leaves,[15] voacangine and voacamine from bark,[16] and vobtusine from roots.[17] But concerns for the preservation of plants from which the molecules are derived make it critical to seek alternative sources of these natural products that avoid removal of plant parts, the harvesting of which threatens plant survival and viability. In this regard, seeds may serve as a readily available, renewable source of medicinal indole alkaloids that in and of themselves can be isolated and purified for use in clinical medicine, or provide access to molecular frameworks that can be used in semi-synthetic approaches to generate drugs of interest (e.g., the use of the natural product vincamine for the semisynthesis of vinpocetine for the treatment of cerebrovascular and cognitive disorders).[18] The seeds of *V. africana* are considered the most economically important plant part[15] and have been reported to contain a number of types of compounds, including lipids and terpenes, as well as indole alkaloids. Medicinal natural products such as tabersonine (which has anti-cancer properties) have been isolated from *V. africana* seeds.[19] These compounds have been isolated using various extraction protocols,[17,19−22] in addition to column chromatography[17,19−22] and thin layer chromatography (TLC),[17,21] and structurally characterized by ^{1}H nuclear magnetic resonance (NMR) spectroscopy,[17,19,21,22] ^{13}C NMR spectroscopy,[17,19,21−23] ^{1}H-^{1}H COSY,[21] infrared (IR) spectroscopy,[21] high-resolution mass spectrometry[17,21,22] and gas chromatography−mass spectrometry (GC-MS).[20,24] Once the presence within seeds of compounds of interest is established, a next step would be to develop a method by which to isolate them. To optimize the isolation protocol for the extraction and purification of relevant compounds from seeds, it would be extremely helpful if the spatial distributions within the seed tissue can be determined beforehand, as this would reduce the expense, waste and overuse of solvent, save time, and enable institution of pretreatment steps to avoid the processing of tissues which do not contain the material of interest. However, the locales of *Voacanga* alkaloids within the seed structure have not been reported.

The ability to map the spatial distributions of small molecules within complex matrices, particularly tissues, has enjoyed numerous technological advancements, with one of the most notable and well-developed being matrix-assisted laser desorption/ionization (MALDI) mass spectrometry imaging (MSI),[25] although a number of other methods have also appeared.[25−27] These techniques have facilitated unprecedented access to proteome spatial distributions in particular. For MALDI-MSI analyses, the sample is first coated with a matrix, and this is followed by laser-facilitated desorption of analytes from the surface of the sample, which are then detected by the mass analyzer while the system is under vacuum. Factors critical to the success of the analysis include choice of matrix (which is often accomplished by trial and error and can be very time-consuming to develop); the choice of solvent used for dissolution of the matrix; appropriate application of the matrix such that distortion of the spatial distributions of small molecules is avoided or minimized; sample thickness (for example, the optimal thickness for tissue samples has been found to be 2−6 μm);[28] and the importance of the sample having a uniform flat surface. There are a number of biological materials that cannot be analyzed by MALDI-MSI because of these requirements. In addition, for samples that are rare, the trial and error nature of method development to optimize the acquisition of useful data can preclude the utilization of this approach because not enough sample may be available for method development. If the material is hard and/or brittle (e.g., wood or bone), it can be impossible for it to be prepared in thin enough slices without it breaking apart. Furthermore, if it is porous, the high vacuum required can be achieved only with great difficulty or not at all. For small-molecule analysis in particular, the low molecular weights of the matrices themselves can complicate the detection of m/z values of interest in the low mass range. Also, small molecules may sublime under the high vacuum, precluding their detection in the MALDI-MSI experiment, and the solvent used to solubilize the matrix can distort the spatial distributions of small molecules of interest. A recently developed alternative technique that circumvents several of the aforementioned challenges, and which thereby can enable spatial distribution mapping in a broader range of biological materials, is termed laser ablation direct analysis in real-time imaging−mass spectrometry (LADI-MS). The approach couples a UV laser with an ambient ionization direct analysis in real-time (DART) ion source, interfaced with a time-of-flight (TOF) mass analyzer.[27] The surface of the sample is ablated with the laser to create an ablation plume that is transported via a helium gas flow (through a heated steel transfer line) to the DART gas stream, where the analytes are ionized before entering the mass spectrometer.[27] LADI-MS does not require the use of a matrix or solvent. Samples can be directly analyzed to both preserve the spatial distributions and allow for detection of molecules in the low mass range. It is performed under ambient conditions. Thus, porous samples can readily be analyzed because reduced pressure is not required. MALDI-MSI requires that the surface of the sample be completely flat, and the actual size of the sample is normally restricted to that of a glass slide (approximately 2.5 cm × 7.6 cm). Extremely thin sections of samples are used, and in some cases, samples must be frozen and sliced with a cryostat.[29,30] LADI-MS has a sample chamber of 10 cm × 10 cm, and as such, it can accommodate large and irregularly shaped samples. It also has a 2 cm depth so that thick and uneven surfaces can be analyzed. Recently, it was used to map the spatial distributions of carcinogens in coffee beans, compounds along the biosynthetic pathway leading to tropane alkaloid biosynthesis,[27,31] and small molecules within wood transects[32] whose analysis was previously not possible by conventional methods. In this study, we utilized the LADI-MS approach to determine the spatial distributions within *V. africana* seeds of compounds that may be of interest for further studies of the biological activity of the observed indole alkaloids.

RESULTS AND DISCUSSION

Identification and Detection of Chemical Constituents in *V. africana* Seeds. As a preliminary step to the determination of the spatial distributions of compounds within *V. africana* seeds, and to anticipate what compounds might be

https://doi.org/10.1021/acsomega.3c02464
ACS Omega 2023, 8, 27190−27205

Table 1. Compounds Reported or Detected in *V. africana* Seeds[a]

Entry	Compound	Molecular Formula	Previously Reported in *V. africana* Seeds	Detected by GC-MS in this Work	Detected by DART-HRMS	LADI-MS Ion Image Generated
1	3-Ethylpyridine	C_7H_9N	✓[24]		✓[ABCDE]	
2	1,3-Diethylbenzene	$C_{10}H_{14}$	✓[24]		✓[AB]	
3	α-Pinene	$C_{10}H_{16}$	✓[24]		✓[ABD]	
4	α-Terpineol	$C_{10}H_{18}O$	✓[24]		✓[D]	✓
5	Naphthalene	$C_{10}H_8$	✓[24]		✓[C]	
6	Tetradecanoic acid	$C_{14}H_{28}O_2$	✓[33]	✓[C]	✓[A]	
7	Sesquiterpene Compounds[b]	$C_{15}H_{24}$	✓[24]		✓[AB]	
8	*n*-Hexadecanoic acid	$C_{16}H_{32}O_2$	✓[24, 33]	✓[C]	✓[ABCD]	✓
9	(*Z*,*Z*)-9,12-Octadecadienoic acid	$C_{18}H_{32}O_2$	✓[24]	✓[C]	✓[ABCD]	✓
10	(*E*)-9-Octadecenoic acid	$C_{18}H_{34}O_2$	✓[24]	✓[CF]	✓ [ABCD]	✓
11	(*Z*)-9-Octadecenoic acid	$C_{18}H_{34}O_2$	✓[33]	✓[CF]	✓ [ABCD]	✓
12	Octadecanoic acid	$C_{18}H_{36}O_2$	✓[24, 33]	✓[C]	✓[ABC]	✓
13	Vincamone/Δ^{14}-Vincanol	$C_{19}H_{22}N_2O$	✓[15, 23]		✓[C]	
14	Iboluteine/Iboxygaine	$C_{20}H_{26}N_2O_2$	✓[15, 20]		✓[A]	
15	3-Oxotabersonine/Perakine	$C_{21}H_{22}N_2O_3$	✓[19-20, 22]		✓[ABCE]	✓
16	Compound 1[19]	$C_{21}H_{22}N_2O_5$	✓[19]		✓[CE]	✓
17	Tabersonine	$C_{21}H_{24}N_2O_2$	✓[15, 17, 19, 22, 34]		✓[ABCDE]	✓
18	Deoxoapodine/16-Hydroxytabersonine/Lochnericine/Pachysiphine	$C_{21}H_{24}N_2O_3$	✓[17, 19, 34]		✓[ABCDE]	✓
19	Δ^{14}-Vincamine	$C_{21}H_{24}N_2O_3$	✓[19]	✓[F]	✓[ABCDE]	✓
20	Voacafrine M	$C_{21}H_{24}N_2O_4$	✓[22]		✓[ABCE]	✓
21	(-)-β-Yohimbine/Coronaridine	$C_{21}H_{26}N_2O_2$	✓[20]		✓[ABCE]	✓
22	Vincamine/ψ-Yohimbine/3-*epi*-α-Yohimbine	$C_{21}H_{26}N_2O_3$	✓[18, 20]		✓[ABCE]	
23	Voacafrine N	$C_{21}H_{26}N_2O_4$	✓[22]		✓[BC]	
24	Jerantinine B	$C_{22}H_{26}N_2O_5$	✓[22]		✓[C]	
25	Brassicasterol	$C_{28}H_{46}O$	✓[35]		✓[AB]	
26	Stigmasterol	$C_{29}H_{48}O$	✓[35]		✓[AC]	
27	DL-α-Tocopherol	$C_{29}H_{50}O_2$	✓[35]		✓[A]	
28	Voacafrine D/Voacafrine G	$C_{42}H_{46}N_4O_5$	✓[22]		✓[C]	
29	Vobtusine	$C_{43}H_{50}N_4O_6$	✓[15, 17, 20]		✓[C]	
30	Voacamidine/Voacamine	$C_{43}H_{52}N_4O_5$	✓[15, 17, 20]		✓[C]	
31	Voacaline	$C_{43}H_{52}N_4O_6$	✓[20]		✓[D]	
32	1*H*-Indole-4-carboxaldehyde	C_9H_7NO		✓[F]		
33	Tryptophol	$C_{10}H_{11}NO$		✓[F]	✓[A]	
34	(*E*)-Coniferyl alcohol	$C_{10}H_{12}O_3$		✓[C]	✓[C]	
35	*trans*-Sinapyl alcohol	$C_{11}H_{14}O_4$		✓[F]		
36	Dihydroactinidioide	$C_{11}H_{16}O_2$		✓[F]	✓[ADE]	✓
37	Loliolide	$C_{11}H_{16}O_3$		✓[F]	✓[AC]	
38	Hexahydro-3-(2-methylpropyl)-pyrrolo[1,2-α]pyrazine-1,4-dione	$C_{11}H_{18}N_2O_2$		✓[F]	✓[A]	
39	β-Carboline	$C_{11}H_8N_2$		✓[F]		
40	Harmane	$C_{12}H_{10}N_2$		✓[F]	✓[ABCDE]	✓
41	Acetone anil	$C_{12}H_{15}N$		✓[CF]	✓[C]	
42	*N*-Nitrosocarbazole	$C_{12}H_8N_2O$		✓[F]		
43	3-Methyl-9*H*-carbazol-2-ol	$C_{13}H_{11}NO$		✓[C]	✓[CE]	
44	Dehydrovomifoliol	$C_{13}H_{18}O_3$		✓[F]		
45	2-Anthracenamine	$C_{14}H_{11}N$		✓[F]	✓[BCE]	
46	8-Dimethylamino-1-naphthalenecarboxylic acid methyl ester	$C_{14}H_{15}NO_2$		✓[C]	✓[BC]	
47	1,2,3,4-Tetrahydro-5-methyl-9-acridinamine	$C_{14}H_{16}N_2$		✓[C]		
48	Hexadecanoic acid methyl ester	$C_{17}H_{34}O_2$		✓[C]	✓[E]	
49	(*E*)-2,4-Diphenyl-4-methyl-2-pentene	$C_{18}H_{20}$		✓[C]	✓[C]	✓
50	Triphenylmethanol	$C_{19}H_{16}O$		✓[F]		
51	Decarbomethoxytabersonine	$C_{19}H_{22}N_2$		✓[CF]		
52	*N*,*N*-Dimethyl-6,6-dimethylbicyclo[3.1.1]hept-2-eno[2,3-α]naphthalen-4'-amine	$C_{19}H_{23}N$		✓[F]		
53	Strictamine	$C_{20}H_{22}N_2O_2$		✓[F]	✓[BC]	✓
54	2α,5α-3-Methylene-aspidofractinine	$C_{20}H_{24}N_2$		✓[F]	✓[B]	
55	*N*-[2-(3-Ethyl-1-methyl-9*H*-carbazol-2-yl)ethyl]-*N*-Methylacetamide	$C_{20}H_{24}N_2O$		✓[F]		
56	Tributyl acetylcitrate	$C_{20}H_{34}O_8$		✓[F]	✓[A]	
57	Vobasine	$C_{21}H_{24}N_2O_3$		✓[F]	✓[ABCDE]	✓
58	Akuammidine	$C_{21}H_{24}N_2O_3$		✓[C]	✓[ABCDE]	✓
59	Polyneuridine	$C_{21}H_{24}N_2O_3$		✓[F]	✓[ABCDE]	✓
60	2α,3β,5α,12β,19α,20R-6,7-Didehydro-3-methanol-2,20-cycloaspidospermidine (acetate ester)	$C_{22}H_{26}N_2O_2$		✓[F]		
61	2,6-Di-*tert*-butyl-4-cumylphenol	$C_{23}H_{32}O$		✓[C]	✓[AC]	
62	2,4-Bis(dimethylbenzyl)phenol	$C_{24}H_{26}O$		✓[C]		

[a]Molecules previously reported to be present are indicated in the fourth column with a (√) and include the reference that describes the detection of the indicated molecule. Molecules detected by GC-MS in this work are denoted with a (√) in the fifth column, along with an indication of the type of extract within which the compound was detected (methanol or alkaloid). The observations of masses detected by DART-HRMS that were

https://doi.org/10.1021/acsomega.3c02464
ACS Omega 2023, 8, 27190−27205

Table 1. continued

consistent with the formulas of molecules that have been identified by GC-MS are denoted with a (√) in the sixth column, along with an indication of the material within which the mass was detected (i.e., seed slice, seed powder, or an extract). High-resolution masses detected by LADI-MS, and which corresponded to m/z values for compounds confirmed by GC-MS to be present, or which were consistent with compounds previously reported to be isolated, and for which ion images illustrate their spatial distributions, are listed with (√) in column seven. Green shading indicates the identification is tentative because the structure was not confirmed. Yellow shading indicates that the molecule is of confirmed identity and is newly reported in this work to be in seeds. [A]Detected in a seed slice; [B]detected in seed powder; [C]detected in the methanol extract; [D]detected in the hexanes extract; [E]detected in the methanol extract after defatting with hexanes; and [F]detected in the alkaloid extract;. [b]several sesquiterpenes were reported in the literature and include (+)-δ-cadinene, acoradiene, allo-aromadendrene, *epi*-α-selinene, eudesma-4(14),11-diene, germacrene D, α-cedrene, α-longipinene, β-cedrene, β-farnesene, β-himachalene, β-sesquiphellandrene, and (−)-β-elemene.

detected, a survey of the literature was conducted to determine the compounds that have already been identified to be present in the seeds. The names, molecular formulas, and associated literature references for these molecules are listed in Table 1 as entries 1 through 31, and Supporting Information (SI) Table S1. Entries 1 through 31 in Table 1 are compounds that have been previously reported in the seeds and which were also detected by one or more of the mass spectrometric approaches used in this work. The 59 compounds listed in SI Table S1 are molecules for which no masses consistent with their presence were detected in this work. Among the classes of compounds that have been isolated are terpenes and terpenoids (e.g., Table 1 entries 3, 4), fatty acids (e.g., entries 6, 8−12), and a range of alkaloids (such as entries 13−17), among a range of other miscellaneous molecule types. To determine whether these compounds were present in our *V. africana* seeds, gas chromatography−mass spectrometry (GC-MS) analysis was performed on methanol and alkaloid (i.e., methanol extraction after defatting with hexanes) solvent extracts. Representative chromatograms of the methanol and alkaloid extracts are presented in Figure 1A/B, respectively. The peaks are labeled using Roman numerals with the corresponding identified compounds listed within the tables in the insets. Peaks that were not identified are labeled "u." Of the compounds 1 through 31 in Table 1 that were previously reported to be present in seeds, only entries 6, 8, 9, 11, 12, and 19 (namely, tetradecanoic acid, *n*-hexadecanoic acid, (*Z*,*Z*)-9,12-octadecadienoic acid, (*Z*)-9-octadecenoic acid, octadecanoic acid, and Δ^{14}-vincamine) were tentatively identified based on the matching of their electron ionization (EI) mass spectral fragmentation patterns with those of the corresponding compounds in the National Institute of Standards and Technology (NIST) mass spectral database. In the methanol extract, entries 6, 8, 9, 11, and 12 corresponded to peaks ii, vii, x, xi, and xii in the chromatogram (Figure 1A), and in the alkaloid extract, entry 19 corresponded to peak xxi in the chromatogram (Figure 1B). While the majority of the compounds previously reported to be present in *V. africana* seeds were not observed, 31 other compounds that have not been previously reported in *V. africana* seeds were detected and tentatively identified. These are listed as entries 32 to 62 in Table 1. It is interesting to note that we found 11 reports of the small-molecule constituents in *V. africana* seeds, and comparing these reports, there was very little overlap in the range of compounds detected. In other words, multiple studies reported different compounds. For example, from an ethanol extract, Li et al. observed 3-oxotabersonine, 3α-acetonylvoafrine B, lochnericine, 17,18-dehydrovincamine (Δ^{14}-vincamine), tabersonine, and a new compound with the formula $C_{21}H_{22}N_2O_5$, which were characterized by NMR spectroscopy.[19] On the other hand, Zhao et al. reported an entirely different set of detected molecules (i.e., voacafrines A−N, voafrine A, voafrine B, 3-oxotabersonine, 3α-acetonyltabersonine, 3α-acetonylvoafrine B, 3-oxovoafrine B, and melodinine S), which were detected and characterized using a methanol extraction protocol, column chromatography, and NMR spectroscopy.[22] Given that in these studies, the approaches taken to analyze the seeds were distinct, the observation of a different range of molecules in each case could be a consequence of the differences in experimental methods, which may have favored detection of some compounds over others depending on the protocol used. In addition, it is not unusual to find that the profile of molecules detected in a particular plant part can vary depending on geographic provenance, climate conditions, and/or soil characteristics.[36−38] Prior to the present report, the maximum number of compounds identified in a single study was 27, described in the work by Liu et al. that was focused on detection of sesquiterpenoids.[24] The work reported here utilized two different extraction methods to both optimize the range of molecules detected, and target the investigation of biologically relevant alkaloids in particular. This is likely another reason that a greater range of compounds were detected in this work, compared to other studies. With the exception of Δ^{14}-vincamine, the mass spectral fragmentation pattern matches for detected compounds and those in the NIST EI mass spectral database, rendered as head-to-tail plots, are presented in Suppporting Information Figures S1−S40, while the Δ^{14}-vincamine match was based on the mass spectral data reported by Zhang et al.[39] Figure 2 shows the structures of the identified compounds. These molecules represent both polar and nonpolar compounds and include aromatic alcohols, phenols, sesquiterpene lactones, fatty acids, and numerous alkaloids that have been detected in various *V. africana* plant parts and other species from the Apocyanaceae family such as *Tabernanthe* genus plants (e.g., vobasine,[40] akuammidine,[41] and polyneuridine[42]). In Figure 2, the detected compounds are sorted by class using color coding (i.e., light blue, gray, orange, red, green, yellow, brown, purple, and pink represent fatty acids, carbazoles, sesquiterpenoids, extraneous contaminants, miscellaneous metabolites, carbolines, monoterpene lactones, aromatic alcohols, and indole alkaloids, respectively).

In LADI-MS, the sample is ablated at each x, y-coordinate of the survey area, and the ablation plume that is generated (and which contains the analytes desorbed from the sample surface) is directed via a positive flow of helium gas to the high-resolution time-of-flight mass analyzer that utilizes a DART source for analyte ionization. Because the ion source is DART, any molecules in the ablation plume that are not detectable by DART will not be detectable in the LADI-MS experiment. Accordingly, the seeds were first analyzed by DART-HRMS to determine which of the masses corresponding to compounds

https://doi.org/10.1021/acsomega.3c02464
ACS Omega 2023, 8, 27190−27205

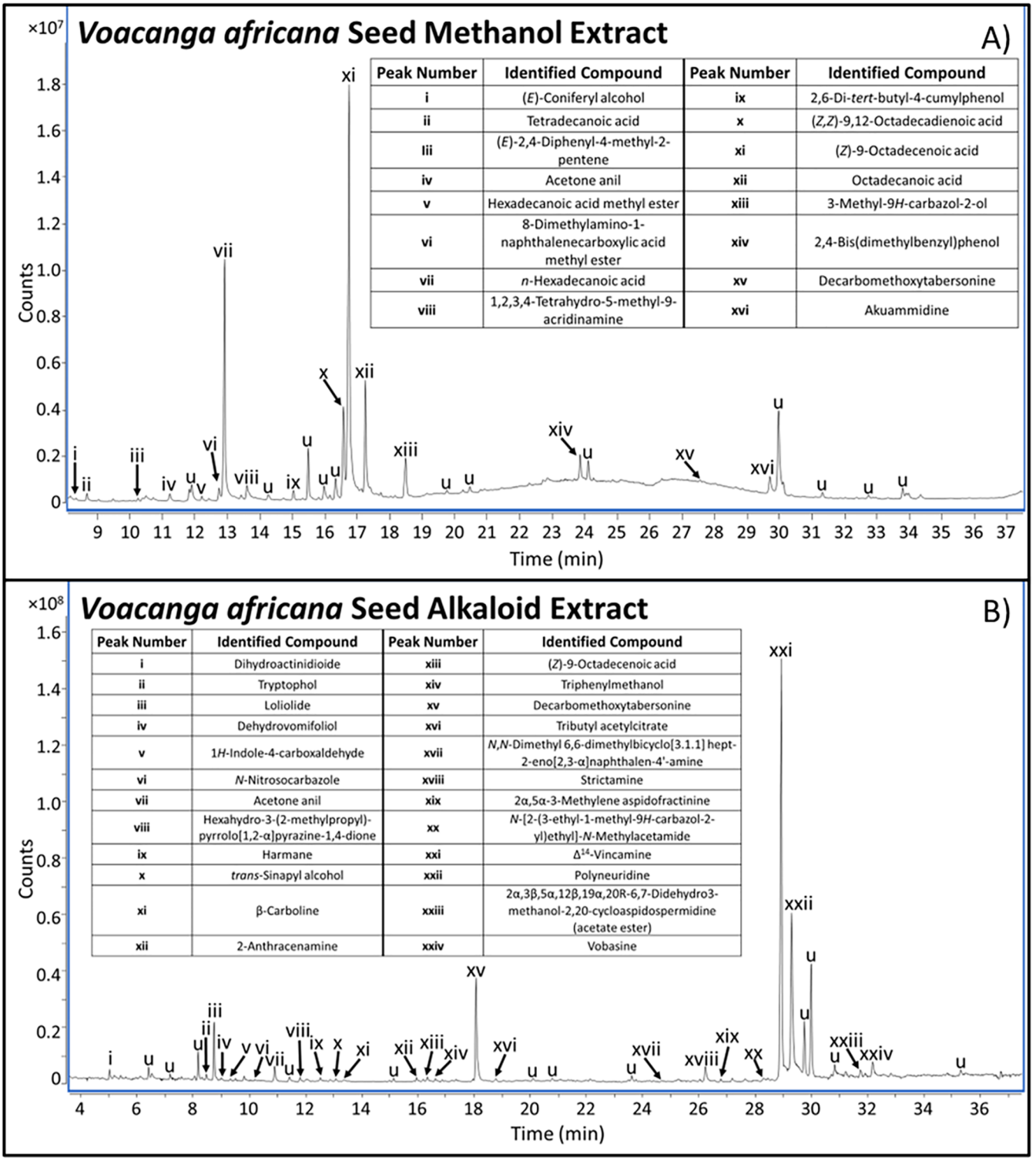

Figure 1. Panel A displays the chromatogram of a *V. africana* methanol extract, and Panel B displays the chromatogram of a *V. africana* alkaloid extract, each analyzed by gas chromatography. The identities of the peaks labeled with Roman numerals are indicated in the tables that appear as insets. Peaks labeled "u" were unidentified.

detected by GC-MS could also be detected by DART-HRMS. The seeds were prepared in two ways for analysis. First, seeds that were cut in half to expose their inner cores were analyzed by suspending them directly into the DART gas stream. Second, seeds were ground to a fine powder, and the seed powder was analyzed directly by DART-HRMS. Representative spectra are presented in Figure 3A/B, respectively. Their corresponding mass spectral data tables are provided in Supporting Information Tables S2 and S3. As the DART ionization mechanism is protonation, and since the analyses were conducted under soft ionization conditions in positive-ion mode, the observed peaks represent the unfragmented protonated precursors of the detected compounds. As anticipated, the mass spectral profiles in Figure 3A/B were

https://doi.org/10.1021/acsomega.3c02464
ACS Omega 2023, 8, 27190−27205

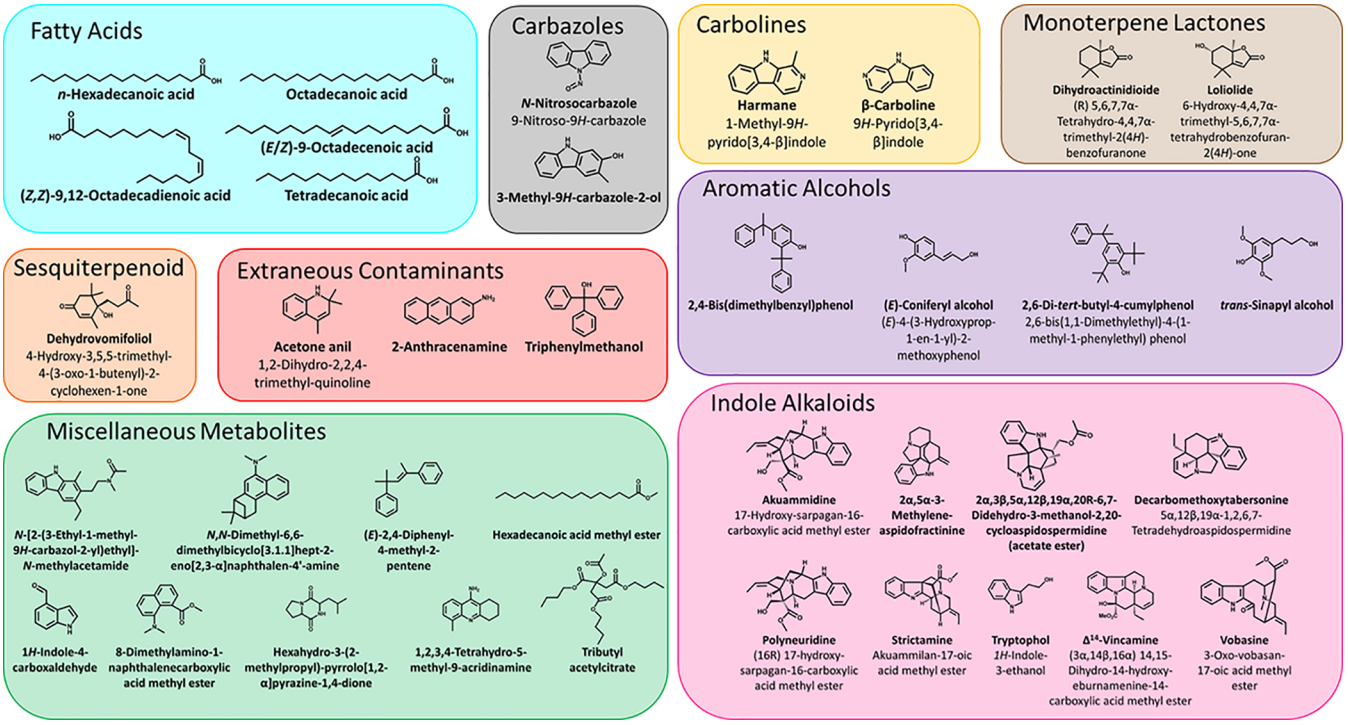

Figure 2. Compounds confirmed to be present in *V. africana* seeds. The detected compounds are sorted by class using color coding (i.e., light blue, gray, orange, red, green, yellow, brown, purple, and pink represent fatty acids, carbazoles, sesquiterpenoids, extraneous contaminants, miscellaneous metabolites, carbolines, monoterpene lactones, aromatic alcohols, and indole alkaloids, respectively).

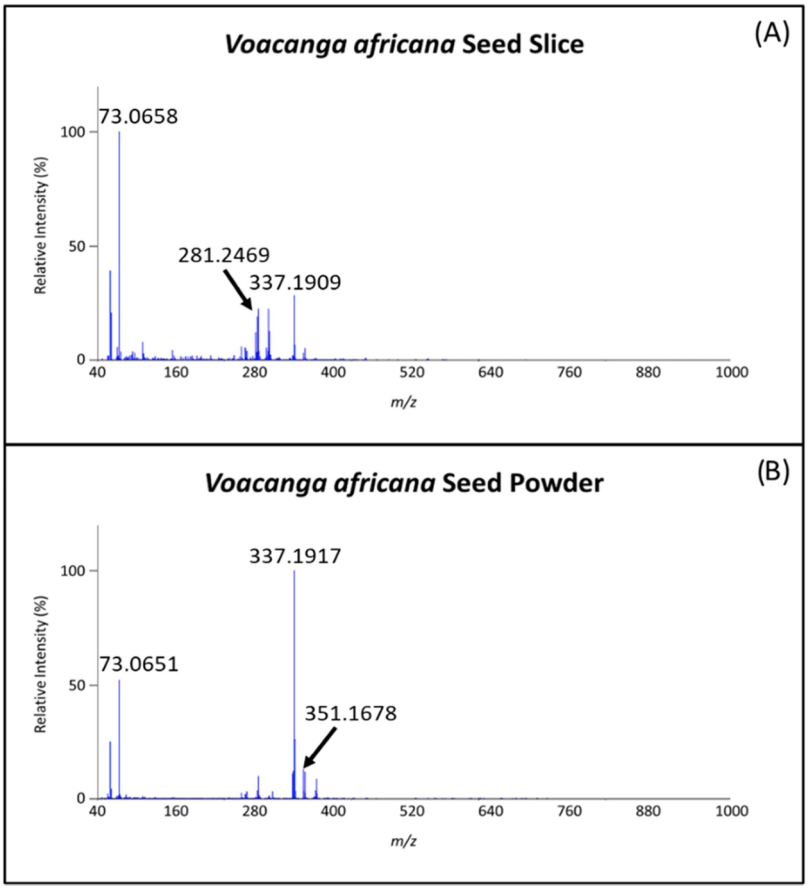

Figure 3. DART high-resolution mass spectra of *V. africana* seeds analyzed in positive-ion mode at 350 °C. Panel A shows the results for a seed slice, and panel B shows the results for the seeds after being ground to a powder.

https://doi.org/10.1021/acsomega.3c02464
ACS Omega 2023, 8, 27190−27205

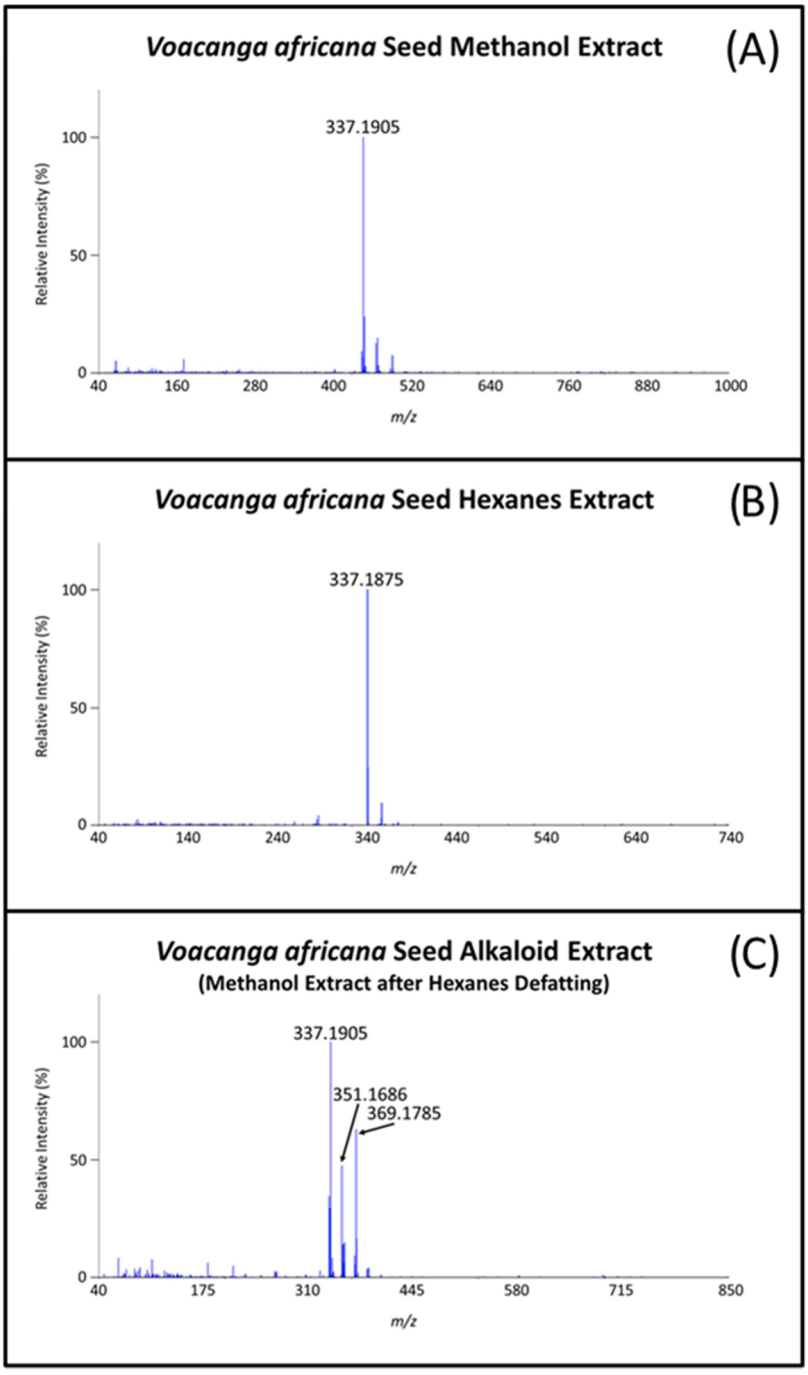

Figure 4. DART high-resolution mass spectra of *V. africana* extracts analyzed in positive-ion mode at 350 °C. Panel A: methanol extract; panel B: hexanes extract; and panel C: alkaloid extract (methanol extract after hexanes defatting).

very similar, although the relative intensities were different, with the latter observation being a consequence of the powder being a more homogeneous sample and the seed being more heterogeneous. What is important to note with DART-HRMS is that because ionization efficiency is based on the proton affinity of the analytes in comparison to that of water, peak intensity is not necessarily correlated to the concentration of the analyte that is present. For example, if two analytes are present in equal concentrations, but one has a much higher proton affinity (e.g., an amine) than the other (e.g., an ester), the ion counts will be far greater for the former because it is more readily ionized than the latter. Therefore, the peak intensities in the spectra in Figure 3A/B cannot be used to infer the relative amounts of the corresponding analytes that are present. DART-HRMS analysis was also performed on methanol, hexanes, and an alkaloid extract of the seeds, with Figure 4 displaying the results. It can be observed that the methanol (panel A) and hexanes extract (panel B) are nearly identical with the same base peak at nominal m/z 337. Using a 1% relative abundance cutoff, the methanol extract had 26 peaks, and the hexanes extract had 13. The alkaloid extract (panel C), which was a methanol extract performed after defatting with hexanes, also has the same base peak, but a number of additional peaks can be detected. Using a 1%

https://doi.org/10.1021/acsomega.3c02464
ACS Omega 2023, 8, 27190−27205

Table 2. Biological Activity and Alternative Sources of Compounds Detected in *V. africana* Seeds[a]

Compound	Biological activity	Alternative sources of seed compounds
akuammidine	–	bark and leaves of *V. grandifolia* (Miq.)[41]
β-carboline	many carbazoles have antibiotic;[48,55] anti-oxidant;[50] and anti-cancer[47] properties	widely reported in plants and first isolated from *Murraya koenigii* Spreng[47]
(*E*)-coniferyl alcohol	–	–
decarbomethoxytabersonine	anti-oxidant;[56] anti-cancer[56]	roots, leaves, and flowers of *Papaver decaisnei*[56]
dehydroyomifoliol	cytotoxic[57]	leaves of *Nitraria sibirica* Pall. (NS)[58]
dihydroactinidioide	anticholinesterase inhibitory activity; prevents amyloid β aggregation[55]	*Arabidopsis* genus;[59] *Camellia sinensis*;[60] *Aspalathus linearis*;[60] *Actinidia polygama*;[55] *Prosopis farcta*[55]
8-dimethylamino-1-naphthalenecarboxylic acid methyl ester	–	*Argania spinosa* L. (Skeels)[61]
2,6-di-*tert*-butyl-4-cumylphenol	high juvenile hormone activity[62]	lobster hemolymph[62]
harmane	anti-anxiety; anti-depressant; anti-platelet; anti-diabetic; acetylcholinesterase and myeloperoxidase inhibition; anti-oxidant; anti-parasitic; hypotensive; alleviation from morphine withdrawal; anti-nociceptive[51]	tea leaves of *Camellia sinensis*;[52] brews of *Coffea arabica*[53]
hexadecanoic acid methyl ester	–	–
hexahydro-3-(2-methylpropyl)-pyrrolo[1,2-α]pyrazine-1,4-dione	anti-cancer[63]	marine bacteria[63]
1*H*-indole-4-carboxaldehyde	–	stems of *Limonia acidissima* L. (Rutaceae)[64]
loliolide	anti-oxidant; anti-fungal; anti-bacterial; anti-cancer[65]	plants;[65] insects;[65] algae[65]
3-methyl-9*H*-carbazole-2-ol	–	*Murraya koenigii*[66]
N-nitrosocarbazole	exterminates nematodes[67]	–
polyneuridine	–	leaves of *Rhyza stricta*;[68] *V. chalotiana* Pierre ex Stapf.;[42] *Alstonia venenata*;[69] *Aspidosperma polyneuron*;[70] *Melodinus suaveolens*[71]
trans-sinapyl alcohol	anti-inflammatory;[72] anti-nociceptive[72]	stem bark of *Magnolia sieboldii*[72]
strictamine	antiviral;[73] cytotoxic;[74] antimicrobial;[75] acetylcholinesterase inhibitor[76]	leaves of *Rhyza stricta*;[74] stem and bark of *Rauvolfia caffra* Sond;[75] *Catharanthus roseus*;[76] *Vinca minor*;[76] leaves and twigs of *Alstonia scholaris*;[73,76]
tributyl acetylcitrate	anti-fungal	*Punica granatuml*[77]
tryptophol	–	needles and seeds of *Pinus sylvestris* L.[78,79]
Δ^{14}-vincamine	vasorelaxant;[43] hypoglycemic[44]	leaves and twigs of *Melodinus hemsleyanus*[43]
vobasine	anti-cancer;[40] cytotoxic;[45] anti-plasmodial[46]	bark of *V. africana*[40]

[a]Presented are reported biological activity and the species and plant parts from which the compounds have been isolated. A dash (–) indicates that no biological activity has been reported. Citations in which the information is referenced are also indicated.

https://doi.org/10.1021/acsomega.3c02464
ACS Omega 2023, 8, 27190−27205

relative abundance cutoff, 85 peaks were detected. This highlights the importance of the defatting step in revealing the presence of compounds in the m/z region of 300−400 which is where a majority of the alkaloids appear. The corresponding mass spectral data tables are presented in Supporting Information Tables S4 through S6.

The high-resolution masses provided by the DART mass spectra enabled assignment of molecular formulas to the detected peaks. Masses observed by DART-HRMS that were correlated to formulas for compounds identified by GC-MS analysis (in both this work and other reports—listed in columns 4 and 5 in Table 1) are indicated in the "Detected by DART-HRMS" column of Table 1 (i.e., column 6). Entries in this column indicate the nature of the material in which the high-resolution mass corresponding to the indicated molecular formula was detected (i.e., a seed slice; pulverized seed (i.e., powder); methanol extract; hexanes extract; or defatted methanol extract).

From the results presented in Table 1, a number of conclusions can be drawn. First, using DART-HRMS and GC-MS, this work was able to confirm the presence of six compounds that have previously been reported in the seeds of *V. africana*, namely, tetradecanoic acid, *n*-hexadecanoic acid, (*Z*,*Z*)-9,12-octadecadienoic acid, octadecanoic acid, and Δ^{14}-vincamine.[19,24,33] 9-Octadecenoic acid was also detected. However, both *E* and *Z* configurations have been reported, and this work did not specifically determine the configuration of the detected compound.[24,33] All six of these compounds have been isolated from other plants, and Δ^{14}-vincamine isolated from the leaves and twigs of *Melodinus hemsleyanus* was shown to have vasorelaxant[43] and hypoglycemic activities.[44]

Second, a total of 31 compounds were newly detected in *V. africana* seeds. These are indicated with yellow shading in Table 1. The structures of these compounds are shown in Figure 2. Some have been reported in *V. africana* and/or other *Voacanga* species but not in their seeds, while others have not been detected in *Voacanga* genus plants but have been observed in other unrelated genera. Most have been discovered to exhibit biological activity, a synopsis of which is presented in Table 2, which lists the compounds, examples of their reported biological activities, and the species and plant parts from which they have been isolated. For example, vobasine has been isolated from *V. africana* bark, and was discovered to have anti-cancer[40,45] and anti-plasmodial activity.[46] *β*-Carboline has a skeletal framework that is the basis of numerous alkaloids widely observed in plants,[47] and many of which have been reported to exhibit various biological properties such as antibiotic,[48,49] anti-oxidant,[50] and anti-cancer activities.[47] Harmane is one such derivative that is known to have anti-anxiety, anti-depressant, anti-platelet, anti-diabetic, acetylcholinesterase and myeloperoxidase inhibitory, anti-oxidant, anti-parasitic, hypotensive, and anti-nociceptive properties.[51] It has been found in *Camellia sinensis* tea leaves,[52] as well as brews of coffee (*Coffea arabica*),[53] but has not previously been reported in *V. africana*.

Third, a number of the detected compounds are not known to be natural products and therefore may be extraneous contaminants. These include 2-anthracenamine (a volatile reported to be released in the decomposition of pig remains);[54] acetone anil; triphenylmethanol; 2*α*,5*α*-3-methylene aspidofractinine (a reported constituent of landfill leachate);[80] 2,4-bis-(dimethylbenzyl)phenol (a ubiquitous compound used in plastics and consumer products);[81] *N*-[2-(3-ethyl-1-methyl-9*H*-carbazol-2-yl)ethyl]-*N*-methylacetamide (which has been identified in oil shale);[82] *N*,*N*-dimethyl-6,6-dimethylbicyclo[3.1.1]hept-2-eno[2,3-*α*]naphthalen-4′-amine; (*E*)-2,4-diphenyl-4-methyl-2-pentene; and 2*α*,3*β*,5*α*,12*β*,19*α*,20R-6,7-didehydro-3-methanol-2,20-cyclo-aspidospermidine (acetate ester).

Fourth, a number of compounds with high-resolution masses consistent with molecules previously detected in *V. africana* seeds, but whose presence could not be confirmed in this study by GC-MS, as we did not detect them in our GC-MS experiments, were observed by DART-HRMS. Some of the corresponding formulas were associated with only a single previously identified molecule, while others were associated with multiple isomers. For example, while there are numerous monoterpenes with the formulas $C_{10}H_{16}$ and $C_{10}H_{18}O$, only one molecule corresponding to each of these formulas has been reported in *V. africana*, namely, *α*-pinene and *α*-terpineol, respectively. Iboluteine, tabersonine, voacafrine M, (−)-*β*-yohimbine, voacafrine N, jerantinine B, brassicasterol, stigmasterol, DL-*α*-tocopherol, vobtusine, voacaline, and 3-ethylpyridine have all been isolated from *V. africana* seeds in previous work,[15,17,19,20,22,24,34,35] and their respective protonated monoisotopic masses were detected. Li et al. identified a compound with the formula $C_{21}H_{22}N_2O_5$ in seeds (Table 1 entry 16),[19] and its corresponding formula in protonated form was observed here by DART-HRMS. The mass corresponding to the chemical formula $C_{15}H_{24}$ was observed and represents a number of possible sesquiterpenes that have previously been detected in *V. africana* seeds,[24] including (+)-*δ*-cadinene, acoradiene, allo-aromadendrene, *epi*-*α*-selinene, eudesma-4(14),11-diene, germacrene D, *α*-cedrene, *α*-longipinene, *β*-cedrene, *β*-farnesene, *β*-himachalene, *β*-sesquiphellandrene, and (−)-*β*-elemene. Both vincamone and Δ^{14}-vincanol, which are isomers with the formula $C_{19}H_{22}N_2O$,[15,23] have been reported in *V. africana* seeds, and a corresponding protonated mass was detected by DART-HRMS. The protonated forms of the formulas associated with the isomers 3-oxotabersonine and perakine ($C_{21}H_{22}N_2O_3$), both of which have been isolated from *V. africana* seeds,[19,20,22] were also detected. Through our GC-MS analyses (see Table 1, column 5), we identified the formula $C_{21}H_{24}N_2O_3$ to correspond to the compounds vobasine, akuammidine, polyneuridine, and Δ^{14}-vincamine. It should be noted, however, that multiple other compounds that have this same formula have been detected in *V. africana* seeds, although we did not observe them in the present work. These include deoxoapodine, 16-hydroxytabersonine, lochnericine, and pachysiphine (see entry 18 in Table 1).[17,19,34] DART-HRMS detected masses consistent with the formulas $C_{21}H_{26}N_2O_3$ (corresponding to vincamine, *ψ*-yohimbine, and 3-*epi*-*α*-yohimbine);[18,20] $C_{42}H_{46}N_4O_5$ (corresponding to voacafrine D and voacafrine G);[22] and $C_{43}H_{52}N_4O_6$ (corresponding to voacamidine and voacamine)[15,17,20] were also detected. Further isolation and structural characterization work will be required to confirm the identities of the formulas deduced from the monoisotopic masses.

Seed Tissue Analysis. Having tentatively identified numerous compounds of varying biological activity and importance, we next investigated their locales within the *V. africana* seed tissue. Multiple *V. africana* seeds were imaged using LADI-MS to verify that the observations made were consistent across multiple individuals. Seeds were cut trans-

https://doi.org/10.1021/acsomega.3c02464
ACS Omega 2023, 8, 27190−27205

versely to reveal the inner anatomy of the cross section, the surface of which was surveyed by LADI-MS. Figure 5 displays a light microscopy image of a representative seed. Highlighted are some of its anatomical features, including the outer seed coat, the endosperm, and the embryo.

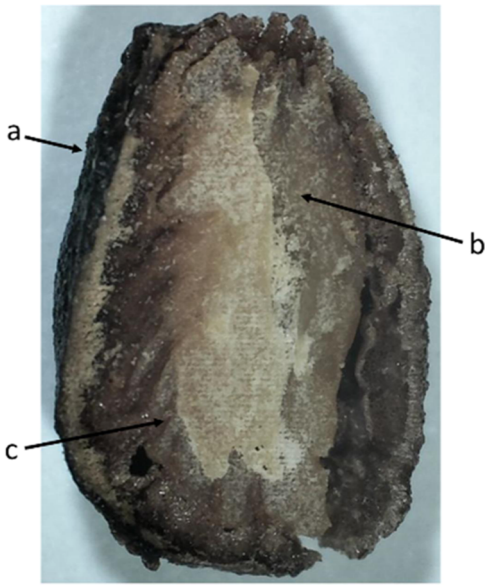

Figure 5. *V. africana* seed transect analyzed by LADI-MS. Highlighted are the outer seed coat (a), the embryo (b), and the endosperm (c).

Ion Images Acquired Using LADI-MS. Figure 6 (panels A through I) shows the ion images reflecting the spatial distributions of the compounds confirmed to be present in *V. africana* seeds by DART-HRMS and GC-MS (entries 8−12, 19, 36, 40, 49, 53, and 57−59 in Table 1), with their molecular structures shown in Figure 2. Figure 7 displays the ion images for *m*/*z* values (with their corresponding formulas) whose structures were not confirmed but whose chemical formulas are consistent with molecules previously reported in *V. africana* seeds (entries 4, 15−17, 20, and 21 in Table 1). The images shown in Figures 6 and 7 were derived from the seed whose light microscopy image is shown in Figure 5. Each image contains a color scale bar in which white and yellow indicate high intensities and brown low or zero intensity. A size scale bar representing 100 μm is also shown. The minor horizontal shadows that appear in some images (such as in Figures 6C/D/H and 7A/C) are a result of the uneven surface of the sample. It should also be noted that because the ion source is DART, the peak intensities do not necessarily represent the relative concentrations of the detected ions and therefore the differences in the intensity scales between ion images do not necessarily indicate the relative levels of the detected ions.

Panels A, B, and C in Figure 6 show the spatial distributions of dihydroactinidioide, harmane, and (*E*)-2,4-dipheny-4-methyl-2-pentene, respectively. The high similarity of the ion images is a consequence of the fact that these molecules are localized to the same area. Although these three compounds represent multiple compound classes, they are all primarily located at the periphery of the endosperm. Panels D through G represent the four fatty acids identified, namely, *n*-hexadecanoic acid, (*Z*,*Z*)-9,12-octadecadienoic acid, (*E*/*Z*)-9-octadece-

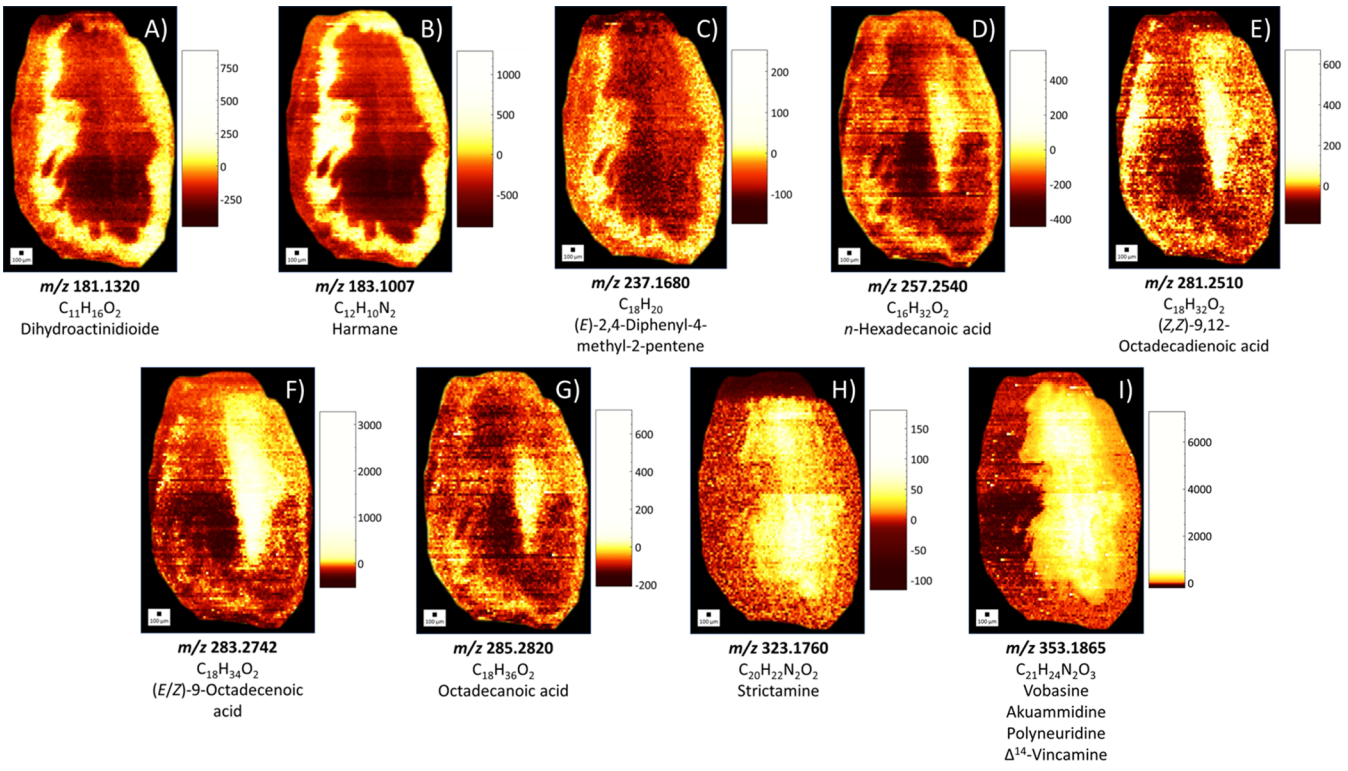

Figure 6. LADI-MS ion images of compounds confirmed to be present in *V. africana* seeds. The protonated monoisotopic masses detected in the DART mass spectra that were used to generate the images are listed. For each, there is a corresponding chemical formula and the identified compound(s) associated with the formula. The images are sorted by organelle presence. Panels A, B, and C highlight the outer portion of the endosperm. Panels D, E, F, and G highlight the embryo. Panels H and I highlight the inner portion of the endosperm.

https://doi.org/10.1021/acsomega.3c02464
ACS Omega 2023, 8, 27190−27205

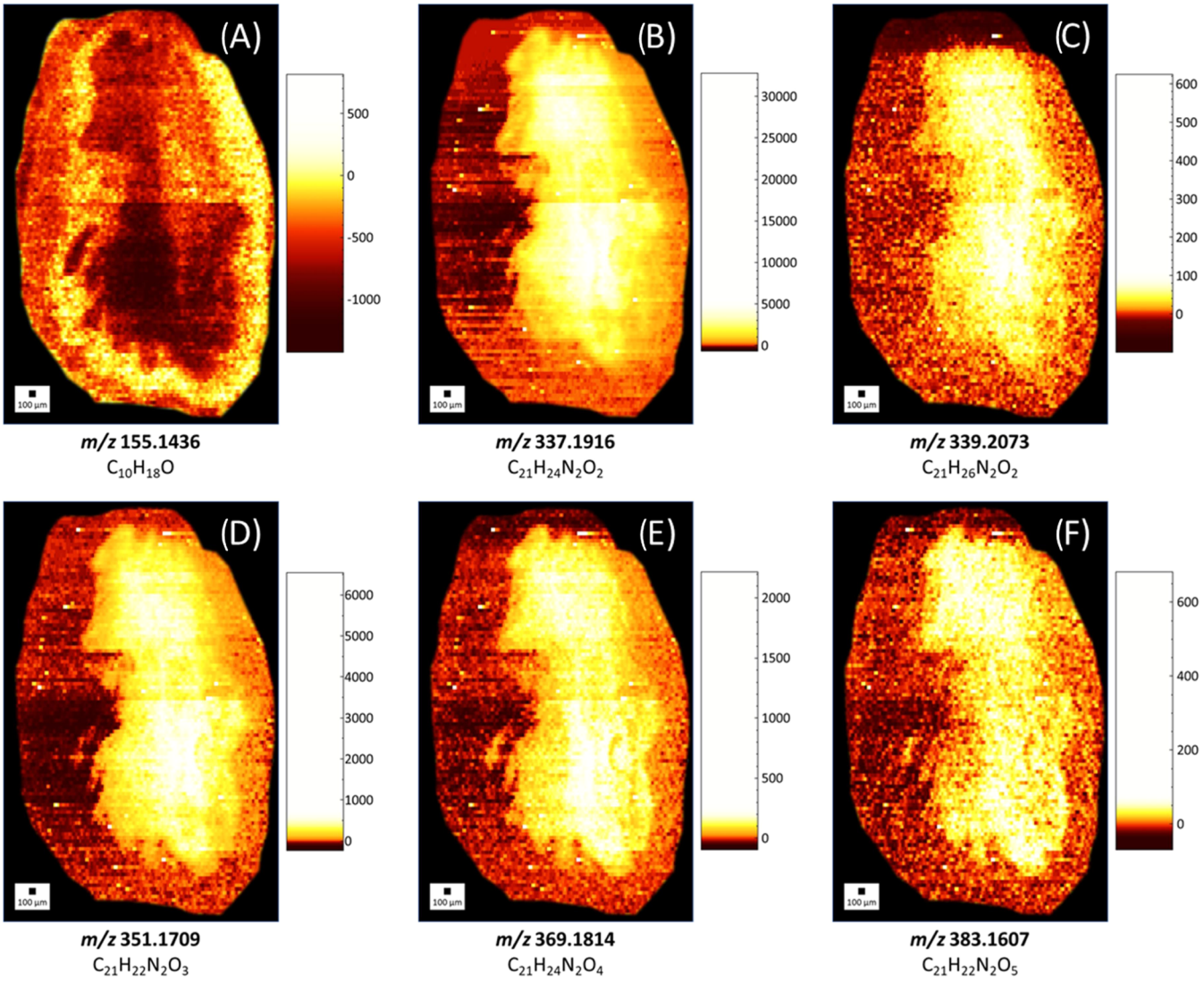

Figure 7. LADI-MS ion images of compounds confirmed to be in *V. africana* seeds. The protonated monoisotopic mass detected in the DART mass spectra that was used to generate the image is listed. For each, a corresponding chemical formula is listed. The images are sorted by organelle presence. Panel A highlights the outer portion of the endosperm. Panels B, C, D, E, and F highlight the inner portion of the endosperm.

noic acid, and octadecanoic acid, respectively. The ion images show that they are located primarily in the embryo. All of these compounds have previously been found in seed embryos,[83] which is unsurprising, given that the embryo uses fatty acids as nutrients. Panels H and I represent alkaloids which were distributed across the entire endosperm with higher levels in the interior. Panel H was identified as strictamine, while the ion image in Panel I corresponding to m/z 353.1865 could be any one of four compounds, namely vobasine, akuammidine, polyneuridine, and Δ^{14}-vincamine. As they are isomers, DART-HRMS cannot differentiate between them, and the absence of authentic standards precluded the possibility of confirming their identities based on comparison with the fragmentation patterns of authentic standards. However, our GC-MS analyses revealed their presence. In any case, these alkaloids appear localized to the same region.

Figure 7 highlights m/z values detected by LADI-MS that have chemical formulas that match with compounds that have been previously reported in *V. africana* seeds. Panel A displays the ion image of m/z 155.1436. This is localized in the outer area of the endosperm and represents the chemical formula $C_{10}H_{18}O$, which is consistent with α-terpineol and other monoterpenoids. Panels B, C, D, E, and F highlight ions that are centralized in the inner portion of the endosperm (m/z 337.1916, 339.2073, 351.1709, 369.1814, and 383.1607, respectively). These masses correspond to the chemical formulas $C_{21}H_{24}N_2O_2$ (i.e., tabersonine), $C_{21}H_{26}N_2O_2$ (i.e., (−)-β-yohimbine), $C_{21}H_{22}N_2O_3$ (i.e., vincamine, ψ-yohimbine, 3-*epi*-α-yohimbine), $C_{21}H_{24}N_2O_4$ (i.e., voacafrine M), and $C_{21}H_{22}N_2O_5$ (i.e., Compound 1[19]), respectively. As can be seen in the subset of images presented in Supporting Information Figure S41 showing the results for a different seed, the locales of the indicated ions are consistent with the results shown here. For example, the distributions of m/z 339.2073 and 369.1814 in the seed shown in Figure S41 are similar to those shown for the same m/z values in Figure 7 (see panels C and E).

In summary, we were able to map the locations within seed tissue of several compounds that had previously been reported in *V. africana* seeds but whose locales were not known. We were also able to detect and map the locations of several additional compounds that had not previously been reported

https://doi.org/10.1021/acsomega.3c02464
ACS Omega 2023, 8, 27190−27205

in *V. africana* seeds, many of which are of interest because of their biological activity (Table 2). Their potential therapeutic utility, scarcity, and interesting molecular frameworks have made them targets of organic synthesis. For example, strictamine, vobasine, akuammidine, polyneuridine, and Δ^{14}-vincamine all have biological activity (as discussed above—see Table 2). Multiple approaches have been devised for the asymmetric synthesis of strictamine[84−87] and polyneuridine,[88−90] but reports of the synthesis of vobasine,[91] akuammidine,[90] and Δ^{14}-vincamine[92] are limited. The general inaccessibility of these compounds makes the study of their potential therapeutic utility very challenging or impossible. The results presented here indicate that *V. africana* seeds can be a source of these compounds. By leveraging the spatial distribution information that can be readily revealed by LADI-MS, it is possible to develop more efficient and targeted natural product isolation protocols for compounds of interest such as those detected here. Furthermore, the utilization of seeds as a source of valuable natural products (as opposed to roots, bark, or leaves) has the advantage of promoting preservation of biodiversity and environmental stewardship, as it prevents the destruction of plants, while also allowing alkaloids and other compounds of interest to be isolated.

CONCLUSIONS

Using GC-MS, six compounds previously reported in *V. africana* seeds, ranging from fatty acids, alkaloids, and terpenes, were confirmed to be present namely, tetradecanoic acid, *n*-hexadecanoic acid, (*Z*,*Z*)-9,12-octadecadienoic acid, (*Z*)-9-octadecenoic acid, octadecanoic acid, and Δ^{14}-vincamine. In addition, 31 additional compounds falling under the classes of carbazoles, sesquiterpenoids, carbolines, monoterpene lactones, aromatic alcohols, indole alkaloids, extraneous contaminants, and miscellaneous metabolites were detected in *V. africana* seeds for the first time. The spatial distributions of several of these compounds, which could not be determined by MALDI-MSI, were readily revealed by LADI-MS. Fatty acids were primarily located in the embryo. The alkaloids that were detected included strictamine, akuammidine, polyneuridine, vobasine, and Δ^{14}-vincamine and were found to span the inner portion of the seed endosperm. A range of other compounds representing several classes (such as the monoterpene lactone dihydroactinidioide, the carboline harmane, and the metabolite (*E*)-2,4-dipheny-4-methyl-2-pentene) were localized to the perimeter of the endosperm. The findings support the use of LADI-MS for the mapping of small molecules to anatomical features of plant tissue in such a way as to enable more efficient and targeted isolation of compounds of interest. This would be especially important for natural products of economic importance and supports the utilization of seeds as a rich, renewable source of biologically active compounds.

MATERIALS AND METHODS

Seeds. Five ounces of *Voacanga africana* seeds were purchased from World Seed Supply (Mastic Beach, NY).

Extraction of *V. africana* Compounds. *Methanol Extraction.* To isolate the constituent compounds in *V. africana* seeds, 100 mg of seeds were crushed with a mortar and pestle. The powder was placed in a 2 mL Eppendorf tube, and 1.5 mL of methanol (Pharmco-Aaper, Brookfield, CT) was added. The solution was sonicated for 20 min using an FS30 sonic cleaner (Fisher Scientific, Pittsburgh, PA) and centrifuged, and the supernatant was filtered through a cotton plug (Walmart, Albany, NY) lodged within a Pasteur pipette (VWR, Radnor, PA). The filtrate was collected in a 1 dram vial (VWR, Radnor, PA). The extraction process was repeated twice more, and the supernatants were combined. The solvent was then evaporated to dryness while wrapped in aluminum foil to protect the sample from light. The sample was then resuspended in 2 mL of methanol, and 1 mL of the solution was filtered through a cotton plug into a GC vial (Agilent, Santa Clara, CA) for analysis.

Alkaloid Extraction. Adapting the protocol published by Krengel et al. for the extraction of alkaloids,[93] 1.7 g of seeds were ground with a mortar and pestle and transferred to a glass scintillation vial (Fisher Scientific, Pittsburgh, PA). To this, 3.5 mL of hexanes (Pharmco-Aaper, Brookfield, CT) was added, and the solution was sonicated for 30 min. The solvent was transferred using a Pasteur pipette to a separate scintillation vial. This extraction was repeated twice more, and all of the hexanes extracts were combined. To the seed powder residue, 3.5 mL of methanol was added, and the solution was sonicated for 30 min. The solvent was transferred to a scintillation vial, and the methanol extraction was repeated twice more, each time combining the methanol extracts. The solvent was then evaporated and resuspended in 0.001 M HCl (Sigma-Aldrich, St. Louis, MO). The solution was filtered through a cotton plug lodged within a Pasteur pipette, and the pH of the filtrate was adjusted to 10 using a 10% solution of NaOH (Sigma-Aldrich, St. Louis, MO). The organic layer was extracted thrice using CH_2Cl_2 (Pharmco-Aaper, Brookfield, CT) and dried with Na_2SO_4. The solution was decanted, and the solvent was subsequently evaporated off.

GC-MS Analysis. Identification of compounds was performed by GC-MS using a 7890B gas chromatogram interfaced with a 5977B mass spectrometer (Agilent, Santa Clara, CA) coupled to a GERSTEL multipurpose sampler (MPS) (GERSTEL, Linthicum, MD). The column used was a DB-5MS UI (30 m, 0.25 mm I.D., 0.25 μm) (Agilent, Santa Clara, CA). The oven had an initial temperature of 150 °C that was increased at a rate of 4 °C/min until reaching 300 °C. The inlet temperature was 300 °C, the helium flow rate was 1 mL/min, and 1 μL of the sample was injected. The mass spectrometer parameters were as follows: the ionization mode was electron ionization (EI), and the ion source temperature was 230 °C. For the methanol extract samples, 1 mL of solution was transferred to a GC vial (Agilent, Santa Clara, CA). A split of 1:5 was used, the m/z range was 50−500, and the solvent delay was 8 min. For the alkaloid extract samples, the residue was resuspended in chloroform (Sigma-Aldrich, St. Louis, MO), filtered, and transferred to a GC vial. A split of 1:10 was used, the m/z range was 50−600, and the solvent delay was 3.5 min. Data processing, which included automatic and manual peak integration, was performed using MassHunter Qualitative Analysis Software (Agilent, Santa Clara, CA).

Seed Preparation for Mass Spectral Analysis. Using a razor blade, *V. africana* seeds were sliced in half, transverse wise. In addition, seeds were ground with a mortar and pestle to generate a homogeneous powder. For LADI-MS analysis, the seed halves were mounted separately into the laser ablation airtight sample chamber using Loctite Fun Tak mounting putty (Westlake, OH) with the interior face of the seed exposed.

DART-HRMS Analysis. For mass spectral analysis, a direct analysis in real-time (DART) standardized voltage and

https://doi.org/10.1021/acsomega.3c02464
ACS Omega 2023, 8, 27190−27205

pressure (SVP) ion source (IonSense, Saugus, MA) coupled to an AccuTOF high-resolution mass spectrometer (JEOL USA, Inc., Peabody, MA) was used. This instrument has a resolving power of 6000 full width at half-maximum (FWHM) and a mass accuracy of 5 millimass units (mmu). The analyses were performed under soft ionization conditions in positive-ion mode at 350 °C. The helium gas (Airgas, Albany, NY) had a flow rate of 2.0 L/min. The mass spectrometer setting for orifice 1 was 20 V, the orifice 2 and ring lens were 5 V, and the peak voltage was 400 V to acquire spectra within the m/z range 40−1000.

To analyze the seed halves directly, the sample was held with tweezers and suspended in the DART gas stream for 5 to 10 s. To analyze the seed powder, the closed end of a melting point capillary tube (VWR, Radnor, PA) was dipped into the powder, and the coated surface of the capillary was introduced into the open-air space between the ion source and mass spectrometer inlet. The methanol extract, whose preparation for GC-MS analysis was described above, was analyzed by DART-HRMS. The hexanes extract that was analyzed by DART-HRMS was the product of the first extraction step of the preparation of the alkaloid extract for GC-MS. Before the alkaloid extract was evaporated and resuspended using aqueous HCl (described above), it was analyzed after defatting with hexanes. For all solvent extractions, the closed end of a melting point capillary tube was dipped into the solution and then suspended in the open-air space between the ion source and mass spectrometer inlet. Each mass spectrum consisted of five measurements that were averaged to generate a single spectrum. Polyethylene glycol (PEG) 600 (Sigma-Aldrich, St. Louis, MO) was used as a mass calibrant. TSSPro3 software (Shrader Analytical, Grosse Pointe, MI) was used for the processing of the mass spectra, including calibration, averaging, background subtraction, and centroiding. The data were stored as text files, and Mass Mountaineer software (RBC Software, Portsmouth, NH) was used for mass spectral analysis and elemental composition determination.

LADI-MS Analysis. The setup of the laser ablation imaging system termed laser ablation direct analysis in real-time imaging−mass spectrometry (LADI-MS) has previously been described.[27] In brief, an Elemental Scientific Laser NWR213 laser imaging system (ESL, Bozeman, MT) is coupled to a DART-SVP ion source (IonSense, Saugus, MA) and JEOL AccuTOF mass spectrometer (JEOL USA, Inc., Peabody, MA) using heated stainless steel tubing and a glass T to acquire ion images. The laser parameters were optimized on one of the seed halves. The fluence was set to approximately 3.6 J/cm^2, the spot size was 60 × 60 μm^2, the helium gas (Airgas, Albany, NY) flow was 725 mL/min, the frequency was 20 Hz, the warm-up time of the laser was set to 5 s, and the washout time was set to 2 s. The scan speed was 55 μm/s and is determined by the spot size. Using a scan of speed 5 μm/s less than the spot size was found to be optimal not only to ensure full surface ablation but also to prevent excessive ablation of the sample in one spot. For the mass spectra, the data were acquired in positive-ion mode at 350 °C using a m/z range of 80−800. The orifice 1 voltage was set to 20 V, and the orifice 2 and ring lens voltages were both 5 V. The helium flow to the DART-SVP ion source was 2.0 L/min, and the ion guide voltage was set to 800 V to detect ions over m/z 80. The spectrum recording interval was set to 0.6 s per scan. PEG 600 was used for calibration of the mass spectra. TSSPro3 software (Shrader Analytical, Grosse Pointe, MI) was used for the data processing of the mass spectra, including calibration, centroiding, and generation of reconstructed ion chromatograms (RICs) for each ion of interest. The RICs were then exported to Microsoft Excel files, the headings were changed to an Agilent file format, and the data were imported into Iolite imaging software (University of Melbourne, Australia) (https://iolite.xyz). This software enables the coupling of the mass spectral data to the file created by the laser system to generate ion images. The images were generated using the empirical cumulative distribution function (ECDF) scale with the color gradient "Hot".

■ ASSOCIATED CONTENT

Supporting Information

The Supporting Information is available free of charge at https://pubs.acs.org/doi/10.1021/acsomega.3c02464.

Additional seed compounds reported in the literature but not detected, head-to-tail plots of mass spectra for compound identifications, mass spectral data tables corresponding to DART-HRMS spectra, and additional LADI-MS ion images for other seeds (PDF)

■ AUTHOR INFORMATION

Corresponding Author

Rabi Ann Musah − *Department of Chemistry, University at Albany, State University of New York, Albany, New York 12222, United States;* orcid.org/0000-0002-3135-4130; Email: rmusah@albany.edu

Author

Allix Marie Coon − *Department of Chemistry, University at Albany, State University of New York, Albany, New York 12222, United States;* orcid.org/0000-0003-3933-5804

Complete contact information is available at: https://pubs.acs.org/10.1021/acsomega.3c02464

Notes

The authors declare no competing financial interest.

■ ACKNOWLEDGMENTS

The financial support of the National Science Foundation (grant numbers 1429329 and 1710221) to R.A.M. is gratefully acknowledged.

■ REFERENCES

(1) Keawpradub, N.; Kirby, G. C.; Steele, J. C. P.; Houghton, P. J. Antiplasmodial activity of extracts and alkaloids of three *Alstonia* species from Thailand. *Planta Med.* **1999**, *65*, 690−694.

(2) Zheng, Y. Y.; Shen, N. X.; Liang, Z. Y.; Shen, L.; Chen, M.; Wang, C. Y. Paraherquamide J, a new prenylated indole alkaloid from the marine-derived fungus *Penicillium janthinellum* HK1-6. *Nat. Prod. Res.* **2020**, *34*, 378−384.

(3) Yang, B.; Tao, H.; Lin, X.; Wang, J.; Liao, S.; Dong, J.; Zhou, X.; Liu, Y. Prenylated indole alkaloids and chromone derivatives from the fungus *Penicillium* sp. SCSIO041218. *Tetrahedron.* **2018**, *74*, 77−82.

(4) Dhuguru, J.; Skouta, R. Role of indole scaffolds as pharmacophores in the development of anti-lung cancer agents. *Molecules.* **2020**, *25*, 1615.

(5) Kruczynski, A.; Barret, J.-M.; Etiévant, C.; Colpaert, F.; Fahy, J.; Hill, B. T. Antimitotic and tubulin-interacting properties of vinflunine, a novel fluorinated *Vinca* alkaloid. *Biochem. Pharmacol.* **1998**, *55*, 635−648.

(6) Pope, H. G. *Tabernanthe iboga*: An African narcotic plant of social importance. *Econ. Bot.* **1969**, *23*, 174−184.

(7) Kombian, S. B.; Saleh, T. M.; Fiagbe, N. I.; Chen, X.; Akabutu, J. J.; Buolamwini, J. K.; Pittman, Q. J. Ibogaine and a total alkaloidal extract of *Voacanga africana* modulate neuronal excitability and synaptic transmission in the rat parabrachial nucleus *in vitro*. *Brain. Res. Bull.* **1997**, *44*, 603−610.
(8) Koenig, X.; Hilber, K. The anti-addiction drug ibogaine and the heart: A delicate relation. *Molecules* **2015**, *20*, 2208−2228.
(9) Jamieson, C. S.; Misa, J.; Tang, Y.; Billingsley, J. M. Biosynthesis and synthetic biology of psychoactive natural products. *Chem. Soc. Rev.* **2021**, *50*, 6950−7008.
(10) Taylor, W. I. The Iboga and Voacanga Alkaloids. In *The Alkaloids: Chemistry and Physiology*, Manske, R. H. F., Ed.; Academic Press, 1968; Vol. *11*, pp 79−98.
(11) Jana, G. K.; Paul, S.; Sinha, S. Progress in the synthesis of iboga-alkaloids and their congeners. *Org. Prep. Proced. Int.* **2011**, *43*, 541−573.
(12) Jana, G. K.; Sinha, S. Total synthesis of ibogaine, epiibogaine and their analogues. *Tetrahedron.* **2012**, *68*, 7155−7165.
(13) Zhao, G.; Xie, X.; Sun, H.; Yuan, Z.; Zhong, Z.; Tang, S.; She, X. Bioinspired collective syntheses of iboga-type indole alkaloids. *Org. Lett.* **2016**, *18*, 2447−2450.
(14) Farrow, S. C.; Kamileen, M. O.; Meades, J.; Ameyaw, B.; Xiao, Y.; O'Connor, S. E. Cytochrome P450 and *O*-methyltransferase catalyze the final steps in the biosynthesis of the anti-addictive alkaloid ibogaine from *Tabernanthe iboga*. *J. Biol. Chem.* **2018**, *293*, 13821−13833.
(15) Koroch, A. R.; Juliani, H.; Kulakowski, D.; Arthur, H.; Asante-Dartey, J.; Simon, J. *Voacanga africana*: Chemistry, quality and pharmacological activity. In *ACS Symposium Series*, 2010; Vol. *1021*, pp 363−380.
(16) Smith, B. B.; Mbah, J. A.; Cho-Ngwa, F.; Metuge, J. A.; Efange, S. M. N. Isolation and characterization of filaricidal compounds from the stem bark of *Voacanga africana*, a plant used in the traditional treatment of onchocerciasis in Cameroon. *J. Med. Plants Res.* **2015**, *9*, 471−478.
(17) Kitajima, M.; Iwai, M.; Kogure, N.; Kikura-Hanajiri, R.; Goda, Y.; Takayama, H. Aspidosperma−aspidosperma-type bisindole alkaloids from *Voacanga africana*. *Tetrahedron.* **2013**, *69*, 796−801.
(18) Dubey, A.; Kumar, N.; Mishra, A.; Singh, Y.; Tiwari, M. Review on vinpocetine. *Int. J. Pharm. Life Sci.* **2020**, *11*, 6590−6597.
(19) Li, X.; Deng, Y.; Kang, L.; Chen, L.; Zheng, Z.; Huang, W.; Xu, C.; Kai, G.; Lin, D.; Tong, Q.; Lin, Y.; Ming, Y. Cytotoxic active ingredients from the seeds of *Voacanga africana*. *S. Afr. J. Bot.* **2021**, *137*, 311−319.
(20) Thomas, D. W.; Biemann, K. The alkaloids of *Voacanga africana*. *Lloyd.* **1968**, *31*, 1−8.
(21) Niu, Y.; Yang, C.; Zhou, J.; Huang, S.; Liu, J. Two new compounds with antimicrobial activities from the seeds of *Voacanga africana*. *Phytochem. Lett.* **2016**, *18*, 208−212.
(22) Zhao, Q.; Zhu, W. T.; Ding, X.; Huo, Z. Q.; Donkor, P. O.; Adelakun, T. A.; Hao, X. J.; Zhang, Y. Voacafrines A-N, aspidosperma-type monoterpenoid indole alkaloids from *Voacanga africana* with AChE inhibitory activity. *Phytochemistry* **2021**, *181*, No. 112566.
(23) Pegnyemb, D. E.; Ghogomu, R. T.; Sondengam, B. L. Minor alkaloids from the seeds of *Voacanga africana*. *Fitoterapia* **1999**, *70*, 446−448.
(24) Liu, X.; Yang, D.; Liu, J.; Ren, N. Analysis of essential oils from *Voacanga africana* seeds at different hydrodistillation extraction stages: Chemical composition, antioxidant activity and antimicrobial activity. *Nat. Prod. Res.* **2015**, *29*, 1950−1953.
(25) McDonnell, L. A.; Heeren, R. M. Imaging mass spectrometry. *Mass Spectrom. Rev.* **2007**, *26*, 606−643.
(26) Kiss, A.; Hopfgartner, G. Laser-based methods for the analysis of low molecular weight compounds in biological matrices. *Methods* **2016**, *104*, 142−153.
(27) Fowble, K. L.; Teramoto, K.; Cody, R. B.; Edwards, D.; Guarrera, D.; Musah, R. A. Development of "laser ablation direct analysis in real time imaging" mass spectrometry: Application to spatial distribution mapping of metabolites along the biosynthetic cascade leading to synthesis of atropine and scopolamine in plant tissue. *Anal. Chem.* **2017**, *89*, 3421−3429.
(28) Wang, X.; Zhang, L.; Xiang, Y.; Ye, N.; Liu, K. Systematic study of tissue section thickness for MALDI MS profiling and imaging. *Analyst.* **2023**, *148*, 888−897.
(29) Hu, W.; Han, Y.; Sheng, Y.; Wang, Y.; Pan, Q.; Nie, H. Mass spectrometry imaging for direct visualization of components in plants tissues. *J. Sep. Sci.* **2021**, *44*, 3462−3476.
(30) Bøgeskov Schmidt, F.; Heskes, A. M.; Thinagaran, D.; Lindberg Møller, B.; Jørgensen, K.; Boughton, B. A. Mass spectrometry based imaging of labile glucosides in plants. *Front. Plant Sci.* **2018**, *9*, 892.
(31) Fowble, K. L.; Okuda, K.; Cody, R. B.; Musah, R. A. Spatial distributions of furan and 5-hydroxymethylfurfural in unroasted and roasted *Coffea arabica* beans. *Food Res. Int.* **2019**, *119*, 725−732.
(32) Deklerck, V.; Fowble, K. L.; Coon, A. M.; Espinoza, E. O.; Beeckman, H.; Musah, R. A. Opportunities in phytochemistry, ecophysiology and wood research via laser ablation direct analysis in real time imaging-mass spectrometry. *New Phytol.* **2022**, *234*, 319−331.
(33) Su, Y.-h.; Chen, X.-c.; Bai, K.-k.; Liu, H.-f.; Li, H. GC-MS study on chemical constituents of essential oil from seeds of *Voacanga africana* Stapf. *Chin. J. Pharm. Anal.* **2011**, *31*, 496−498.
(34) Walia, M.; Teijaro, C. N.; Gardner, A.; Tran, T.; Kang, J.; Zhao, S.; O'Connor, S. E.; Courdavault, V.; Andrade, R. B. Synthesis of (−)-melodinine K: A case study of efficiency in natural product synthesis. *J. Nat. Prod.* **2020**, *83*, 2425−2433.
(35) Rafidison, P.; Baillet, A.; Baylocq, D.; Pellerin, F. Study of oil from *Voacanga africana* seeds. *Oleagineux* **1987**, *42*, 299−302.
(36) Liang, Z.; Zhang, J.; Yang, G.; Chen, H.; Zhao, Z. Chemical profiling and histochemical analysis of *Bupleurum marginatum* roots from different growing areas of Hubei province. *Acta Pharm. Sinic. B.* **2013**, *3*, 193−204.
(37) Vasil'eva, I. E.; Shabanova, E. V.; Tsagaan, B.; Bymbaa, K. Elemental profiles of wild *Thymus* L. plants growing in different soil and climate conditions. *Appl. Sci.* **2022**, *12*, 3904.
(38) Sampaio, B. L.; Edrada-Ebel, R.; Da Costa, F. B. Effect of the environment on the secondary metabolic profile of *Tithonia diversifolia*: A model for environmental metabolomics of plants. *Sci. Rep.* **2016**, *6*, No. 29265.
(39) Zhang, Y. W.; Yang, R.; Cheng, Q.; Ofuji, K. Henrycinols A and B, two novel indole alkaloids isolated from *Melodinus henryi* Craib. *Helv. Chim. Acta* **2003**, *86*, 415−419.
(40) Chen, H. M.; Yang, Y. T.; Li, H. X.; Cao, Z. X.; Dan, X. M.; Mei, L.; Guo, D. L.; Song, C. X.; Dai, Y.; Hu, J.; Deng, Y. Cytotoxic monoterpenoid indole alkaloids isolated from the barks of *Voacanga africana* Staph. *Nat. Prod. Res.* **2016**, *30*, 1144−1149.
(41) Hirasawa, Y.; Arai, H.; Rahman, A.; Kusumawati, I.; Zaini, N. C.; Shirota, O.; Morita, H. Voacalgines A−E, new indole alkaloids from *Voacanga grandifolia*. *Tetrahedron.* **2013**, *69*, 10869−10875.
(42) Braekman, J. C.; Tirions-Lampe, M.; Pecher, J. Indole alkaloids. XX. Isolation and structural elucidation of four minor alkaloids from *Voacanga chalotiana* Pierre ex Stapf. *Bull. Soc. Chim. Belg.* **2010**, *78*, 523−538.
(43) Zhang, J.; Liu, Z.-W.; Li, Y.; Wei, C.-J.; Xie, J.; Yuan, M.-F.; Zhang, D.-M.; Ye, W.-C.; Zhang, X.-Q. Structurally diverse indole alkaloids with vasorelaxant activity from *Melodinus hemsleyanus*. *J. Nat. Prod.* **2020**, *83*, 2313−2319.
(44) Yu, Y.; Bao, M. F.; Huang, S. Z.; Wu, J.; Cai, X. H. Vincan- and eburnan-type alkaloids from *Tabernaemontana bovina* and their hypoglycemic activity. *Phytochemistry* **2021**, *190*, No. 112859.
(45) Condello, M.; Pellegrini, E.; Multari, G.; Gallo, F. R.; Meschini, S. Voacamine: Alkaloid with its essential dimeric units to reverse tumor multidrug resistance. *Toxicol. In Vitro.* **2020**, *65*, No. 104819.
(46) Munigunti, R.; Becker, K.; Brun, R.; Calderón, A. I. Determination of antiplasmodial activity and binding affinity of selected natural products towards *Pf*TrxR and *Pf*GR. *Nat. Prod. Commun.* **2013**, *8*, 1934578X1300800.

https://doi.org/10.1021/acsomega.3c02464
ACS Omega 2023, 8, 27190−27205

(47) Aaghaz, S.; Sharma, K.; Jain, R.; Kamal, A. β-Carbolines as potential anticancer agents. *Eur. J. Med. Chem.* **2021**, *216*, No. 113321.
(48) Chakraborty, D. P.; Barman, B. K.; Bose, P. K. On the constitution of murrayanine, a carbazole derivative isolated from *Murraya koenigii* Spreng. *Tetrahedron* **1965**, *21*, 681−685.
(49) Das, K. C.; Chakraborty, D.; Bose, P. Antifungal activity of some constituents of *Murraya koenigii* Spreng. *Experientia* **1965**, *21*, 340.
(50) Francik, R.; Kazek, G.; Cegła, M.; Stepniewski, M. Antioxidant activity of beta-carboline derivatives. *Acta Pol. Pharm.* **2011**, *68*, 185−189.
(51) Khan, H.; Patel, S.; A Kamal, M. Pharmacological and foxicological profile of harmane-β-carboline alkaloid: Friend or foe. *Curr. Drug Metab.* **2017**, *18*, 853−857.
(52) Jiao, Y.; Yan, Y.; He, Z.; Gao, D.; Qin, F.; Lu, M.; Xie, M.; Chen, J.; Zeng, M. Inhibitory effects of catechins on β-carbolines in tea leaves and chemical model systems. *Food Funct.* **2018**, *9*, 3126−3133.
(53) Herraiz, T.; Chaparro, C. Human monoamine oxidase enzyme inhibition by coffee and β-carbolines norharman and harman isolated from coffee. *Life Sci.* **2006**, *78*, 795−802.
(54) Lorenzo, N.; Wan, T.; Harper, R. J.; Hsu, Y.-L.; Chow, M.; Rose, S.; Furton, K. G. Laboratory and field experiments used to identify *Canis lupus* var. *familiaris* active odor signature chemicals from drugs, explosives, and humans. *Anal. Bioanal. Chem.* **2003**, *376*, 1212−1224.
(55) Das, M.; Prakash, S.; Nayak, C.; Thangavel, N.; Singh, S. K.; Manisankar, P.; Devi, K. P. Dihydroactinidiolide, a natural product against Aβ25-35 induced toxicity in Neuro2a cells: Synthesis, *in silico* and *in vitro* studies. *Bioorg. Chem.* **2018**, *81*, 340−349.
(56) Jabbar, A. A.; Abdullah, F. O.; Abdulrahman, K. K.; Galali, Y.; Sardar, A. S. GC-MS analysis of bioactive compounds in methanolic extracts of *Papaver decaisnei* and determination of its antioxidants and anticancer activities. *J. Food Quality.* **2022**, *2022*, No. 1405157.
(57) Ren, Y.; Shen, L.; Zhang, D. W.; Dai, S. J. Two new sesquiterpenoids from *Solanum lyratum* with cytotoxic activities. *Chem. Pharm. Bull.* **2009**, *57*, 408−410.
(58) Yang, Y.; Bakri, M.; Gu, D.; Aisa, H. A. Separation of (S)-dehydrovomifoliol from leaves of *Nitraria sibirica* Pall. by high-speed counter-current chromatography. *J. Liq. Chromatogr. Relat. Technol.* **2013**, *36*, 573−582.
(59) Shumbe, L.; Bott, R.; Havaux, M. Dihydroactinidiolide, a high light-induced β-carotene derivative that can regulate gene expression and photoacclimation in Arabidopsis. *Molecular Plant.* **2014**, *7*, 1248−1251.
(60) del Mar Caja, M.; Preston, C.; Menzel, M.; Kempf, M.; Schreier, P. Online gas chromatography combustion/pyrolysis−isotope ratio mass spectrometry (HRGC-C/P-IRMS) of (±)-dihydroactinidiolide from tea (*Camellia sinensis*) and Rooibos tea (*Aspalathus linearis*). *J. Agr. Food Chem.* **2009**, *57*, 5899−5902.
(61) Rabeh, K.; Sbabou, L.; Rachidi, F.; Ferradouss, A.; Laghmari, G.; Aasfar, A.; Arroussi, H. E.; Ouajdi, M.; Antry, S. E.; Belkadi, B.; Filali-Maltouf, A. Lipidomic profiling of *Argania spinosa* L. (Skeels) following drought stress. *Appl. Biochem. Biotech.* **2023**, *195*, 1781−1799.
(62) Biggers, W. J.; Laufer, H. Identification of juvenile hormone-active alkylphenols in the lobster *Homarus americanus* and in marine sediments. *Biol. Bull.* **2004**, *206*, 13−24.
(63) Lalitha, P.; Veena, V.; Vidhyapriya, P.; Lakshmi, P.; Krishna, R.; Sakthivel, N. Anticancer potential of pyrrole (1, 2, α) pyrazine 1, 4, dione, hexahydro 3-(2-methyl propyl) (PPDHMP) extracted from a new marine bacterium, *Staphylococcus* sp. strain MB30. *Apoptosis* **2016**, *21*, 566−577.
(64) Zarga, M. H. A. Three new simple indole alkaloids from *Limonia acidissima*. *J. Nat. Prod.* **1986**, *49*, 901−904.
(65) Grabarczyk, M.; Wińska, K.; Mączka, W.; Potaniec, B.; Anioł, M. Loliolide-the most ubiquitous lactone. *Folia Biol. Oecol.* **2015**, *11*, 1−8.
(66) Knölker, H.-J.; Reddy, K. R. Isolation and synthesis of biologically active carbazole alkaloids. *Chem. Rev.* **2002**, *102*, 4303−4428.
(67) Mukherjee, D.; Babu, S. Nematicidal effect of *n*-nitroso carbazole. *Environ. Ecol.* **1992**, *10*, 265−268.
(68) Mukhopadhyay, S.; Handy, G. A.; Funayama, S.; Cordell, G. A. Anticancer indole alkaloids of *Rhazya stricta*. *J. Nat. Prod.* **1981**, *44*, 696−700.
(69) Majumder, P.; Basu, A. Alstolenine, 19,20-dihydropolyneuridine, and other minor alkaloids of the leaves of *Alstonia venenata*. *Phytochemistry* **1982**, *21*, 2389.
(70) Antonaccio, L. D.; Pereira, N. A.; Gilbert, B.; Vorbrueggen, H.; Budzikiewicz, H.; Wilson, J. M.; Durham, L. J.; Djerassi, C. Alkaloid studies. XXXIII. Mass spectrometry in structural and stereochemical problems. 6. Polyneuridine, a new alkaloid from *Aspidosperma polyneuron* and some observations on mass spectra of indole alkaloids. *J. Am. Chem. Soc.* **1962**, *84*, 2161−2169.
(71) Zhang, T.-T.; Liu, Z.-W.; Wang, W.-J.; Tong, Y.-B.; Xu, F.-F.; Yuan, J.-Q.; Liu, B.; Zhang, X.-Q.; Ye, W.-C. Alkaloids from *Melodinus suaveolens*. *Heterocycles* **2013**, *87*, 2047−2052.
(72) Choi, J.; Shin, K.-M.; Park, H.-J.; Jung, H.-J.; Kim, H. J.; Lee, Y. S.; Rew, J.-H.; Lee, K.-T. Anti-inflammatory and antinociceptive effects of sinapyl alcohol and its glucoside syringin. *Planta Med.* **2004**, *70*, 1027−1032.
(73) Zhang, L.; Zhang, C.-J.; Zhang, D.-B.; Wen, J.; Zhao, X.-W.; Li, Y.; Gao, K. An unusual indole alkaloid with anti-adenovirus and anti-HSV activities from *Alstonia scholaris*. *Tetrahedron Lett.* **2014**, *55*, 1815−1817.
(74) Abdul-Hameed, Z. H.; Alarif, W. M.; Sobhi, T. R.; Abdel-Lateff, A.; Ayyad, S.-E. N.; Badria, F. A.; Saber, J. New cytotoxic indole-type alkaloids obtained from *Rhazya stricta* leaves. *South Afr. J. Bot.* **2021**, *137*, 298−302.
(75) Bitombo, A. N.; Zintchem, A. A. A.; Atchadé, A. T.; Moni Ndedi, E. D. F.; Khan, A.; Ngono Bikobo, D. S.; Pegnyemb, D. E.; Bochet, C. G. Antimicrobial and cytotoxic activities of indole alkaloids and other constituents from the stem barks of *Rauvolfia caffra* Sond (Apocynaceae). *Nat. Prod. Res.* **2022**, *36*, 1467−1475.
(76) Choudhir, G.; Sharma, S.; Hariprasad, P. A combinatorial approach to screen structurally diverse acetylcholinesterase inhibitory plant secondary metabolites targeting Alzheimer's disease. *J. Biomol. Struct. Dyn.* **2022**, *40*, 11705−11718.
(77) Al-Hashimi, A. G.; Al-Salman, H.; Al-Jadaan, S. A. GC-mass analysis and estimation of pomegranate husks extracts and study of the biological efficacy of compound tri-butyl acetyl citrate as one of the extracts against food fungi. *Orient. J. Chem.* **2018**, *34*, 2089−2097.
(78) Sandberg, G. Biosynthesis and metabolism of indole-3-ethanol and indole-3-acetic acid by *Pinus sylvestris* L. needles. *Planta.* **1984**, *161*, 398−403.
(79) Sandberg, G.; Ernstsen, A.; Hamnede, M. Dynamics of indole-3-acetic acid and indole-3-ethanol during development and germination of *Pinus sylvestris* seeds. *Physiol. Plantarum.* **1987**, *71*, 411−418.
(80) Hu, L.; Zeng, G.; Chen, G.; Dong, H.; Liu, Y.; Wan, J.; Chen, A.; Guo, Z.; Yan, M.; Wu, H.; Yu, Z. Treatment of landfill leachate using immobilized *Phanerochaete chrysosporium* loaded with nitrogen-doped TiO2 nanoparticles. *J. Hazard. Mater.* **2016**, *301*, 106−118.
(81) Zuo, Y.; Zhu, Z. Simultaneous identification and quantification of 4-cumylphenol, 2,4-bis-(dimethylbenzyl)phenol and bisphenol A in prawn *Macrobrachium rosenbergii*. *Chemosphere* **2014**, *107*, 447−453.
(82) Jargalsaikhan, N.; Purevsuren, B.; Bat-Ulzii, B.; Batkhishig, D.; Myagmargerel, B. Investigation of oil shale and its pyrolysis tar from the Uvurjargalant deposit in Mongolia. *Oil Shale* **2022**, *39*, 189−216.
(83) Yu, S.; Du, S.; Yuan, J.; Hu, Y. Fatty acid profile in the seeds and seed tissues of *Paeonia* L. species as new oil plant resources. *Sci. Rep.* **2016**, *6*, No. 26944.
(84) Moreno, J.; Picazo, E.; Morrill, L. A.; Smith, J. M.; Garg, N. K. Enantioselective total syntheses of akuammiline alkaloids (+)-strictamine, (-)-2(S)-cathafoline, and (-)-aspidophylline A. *J. Am. Chem. Soc.* **2016**, *138*, 1162−1165.

https://doi.org/10.1021/acsomega.3c02464
ACS Omega 2023, 8, 27190−27205

(85) Smith, M. W.; Zhou, Z.; Gao, A. X.; Shimbayashi, T.; Snyder, S. A. A 7-step formal asymmetric total synthesis of strictamine via an asymmetric propargylation and metal-mediated cyclization. *Org. Lett.* **2017**, *19*, 1004−1007.
(86) Xiao, T.; Chen, Z.-T.; Deng, L.-F.; Zhang, D.; Liu, X.-Y.; Song, H.; Qin, Y. Formal total synthesis of the akuammiline alkaloid (+)-strictamine. *Chem. Commun.* **2017**, *53*, 12665−12667.
(87) Li, W.; Chen, Z.; Yu, D.; Peng, X.; Wen, G.; Wang, S.; Xue, F.; Liu, X.-Y.; Qin, Y. Asymmetric total syntheses of the akuammiline alkaloids (−)-strictamine and (−)-rhazinoline. *Angew. Chem. Int. Ed.* **2019**, *58*, 6059−6063.
(88) Yin, W.; Ma, J.; Rivas, F. M.; Cook, J. M. First enantiospecific total synthesis of the important biogenetic intermediates, (+)-polyneuridine and (+)-polyneuridine aldehyde, as well as 16-epivellosimine and macusine A. *Org. Lett.* **2007**, *9*, 295−298.
(89) Yin, W.; Kabir, M. S.; Wang, Z.; Rallapalli, S. K.; Ma, J.; Cook, J. M. Enantiospecific total synthesis of the important biogenetic intermediates along the ajmaline pathway, (+)-polyneuridine and (+)-polyneuridine aldehyde, as well as 16-epivellosimine and macusine A. *J. Org. Chem.* **2010**, *75*, 3339−3349.
(90) Chen, W.; Ma, Y.; He, W.; Wu, Y.; Huang, Y.; Zhang, Y.; Tian, H.; Wei, K.; Yang, X.; Zhang, H. Structure units oriented approach towards collective synthesis of sarpagine-ajmaline-koumine type alkaloids. *Nat. Commun.* **2022**, *13*, No. 908.
(91) Rosillo, M.; Gonzalez-Gomez, A.; Dominguez, G.; Perez-Castells, J. Chemistry of biologically active β-carbolines. *Targets Heterocycl. Syst.* **2008**, *12*, 212−257.
(92) Nemes, A.; Szántay, C.; Czibula, L.; Greiner, I. Synthesis of 18-hydroxyvincamines and epoxy-1, 14-secovincamines; A new proof for the aspidospermaneeburnane rearrangement. *Heterocycles* **2007**, *71*, 2347−2362.
(93) Krengel, F.; Herrera Santoyo, J.; Olivera Flores, T. J.; Chávez Ávila, V. M.; Pérez Flores, F. J.; Reyes Chilpa, R. Quantification of anti-addictive alkaloids ibogaine and voacangine in *in vivo*- and *in vitro*-grown plants of two Mexican *Tabernaemontana* species. *Chem. Biodivers.* **2016**, *13*, 1730−1737.

https://doi.org/10.1021/acsomega.3c02464
ACS Omega 2023, 8, 27190−27205